EUROFUSION WPBB-CP(16) 15568

L. Buehler et al.

MHD flow and heat transfer in model geometries for WCLL blankets

Preprint of Paper to be submitted for publication in Proceedings of 29th Symposium on Fusion Technology (SOFT 2016)

This work has been carried out within the framework of the EUROfusion Consortium and has received funding from the Euratom research and training programme 2014-2018 under grant agreement No 633053. The views and opinions expressed herein do not necessarily reflect those of the European Commission.

MHD flow and heat transfer in model geometries for WCLL blankets

L. Bühler, C. Mistrangelo
Karlsruhe Institute of Technology, Postfach 3640, 76021 Karlsruhe, Germany

Abstract

In the water cooled lead lithium (WCLL) blanket liquid lead lithium PbLi is used as breeder, neutron multiplier, and as heat transfer medium. The released heat is removed by water that flows at a pressure of 155 bar through cooling pipes immersed in the liquid-metal pool. In order to withstand disruption-induced forces and water pressure in case of accidental conditions, the breeder zone is stiffened by internal plates that form rectangular ducts in which the liquid metal is confined. Numerical simulations have been performed to predict liquid metal flows in model geometries for WCLL blankets under the influence of external magnetic fields. The flow is driven by an applied pressure gradient and/or by buoyancy due to the presence of volumetric heat sources in the fluid and heat removal at the water-cooled pipes.

Key words: Magnetohydrodynamic (MHD), WCLL blanket, magnetoconvection
PACS:

1. Introduction

One of the liquid metal blanket concepts that is considered as possible option for a DEMOnstration nuclear fusion reactor is the water cooled lead lithium (WCLL) blanket [1]. It consists of modules attached along the poloidal direction to a common back supporting structure housing the liquid metal feeding pipes. Reduced activation ferritic-martensitic steel Eurofer is employed as structural material and liquid lead lithium PbLi serves as tritium breeder, neutron multiplier and heat carrier. Pressurized water (155 bar) cools the blanket structure and the breeding zone. In a design concept developed at CEA a large number of cooling pipes arranged in radial-poloidal planes is immersed in the liquid metal and this results in a complex flow path for the PbLi [2]. Figure 1 shows a sketch of the design. This preliminary design of the equatorial outboard blanket module is taken as reference for the present study. In order to withstand disruption-induced forces and high internal pressure in case of accidental conditions, the breeder zone is reinforced by internal toroidal-poloidal and radial-poloidal stiffeners that form rectangular ducts in which the liquid metal is confined.

In a concept developed at ENEA [3] pipes are arranged in radial-toroidal planes, a case that will be investigated in a separate paper.

In liquid metal blankets magnetohydrodynamic (MHD) effects caused by electromagnetic forces, which result from the interaction of induced electric currents with the plasma confining magnetic field, influence significantly velocity and temperature distribution. In order to assess the impact of these MHD phenomena on flow distribution and heat transfer in the WCLL blanket concept, numerical investigations are carried out to study MHD flows in simplified fundamental geometries with relevance to WCLL blankets. MHD flows are driven by applied pressure gradients or by buoyancy forces caused by non-uniform thermal conditions, due to imposed volumetric heat sources and heat removal by cooling pipes. Studies performed to analyze liq-

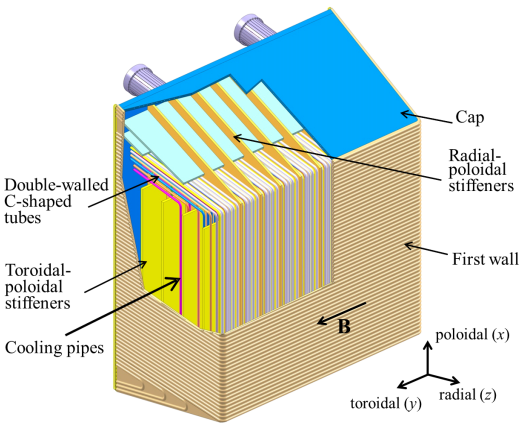

Fig. 1. WCLL blanket according to a design concept developed by CEA [2].

uid metal convective flows for helium cooled lead lithium (HCLL) blankets show that convective phenomena can become very important and they may significantly modify the velocity distribution in the blanket and related heat transfer performance [4] [5]. Even if the geometric arrangement in the WCLL and HCLL blanket is different, it is expected that also in the former one buoyant forces will have a significant influence on MHD flow distribution in the breeding zone. Moreover, due to the presence of cooling tubes, the liquid metal path could become pretty complex. Due to the early stage of the development of the cooling scheme in the breeding region of a DEMO WCLL blanket very few studies are available on such a subject. To the best of our knowledge no numerical investigation exists about MHD buoyant flows in the proposed configuration with cooling pipes. The aim of the present study is to get insight in the MHD flow distribution and in convective motions that result from the non-isothermal operating conditions in WCLL blanket-related geometries. As a first step, fundamental buoyant MHD flows are considered in a model geometry of rectangular cross section, filled with liquid metal heated by a volumetric thermal source, in which one cooling pipe is inserted for heat removal. It is assumed that the axial length is long enough that the flow adjusts to fully developed thermal and hydraulic conditions. The simplified model-problem, as shown in Fig. 2, aims at getting insight in details of MHD flows around obstacles (cooling pipes) with heat transfer and buoyancy. Of particular interest is the closure of current paths and the formation of internal layers tangential to the cooling pipe and parallel to the applied magnetic field. For isothermal conditions the problem has some similarity with MHD flows in concentric circular pipes treated initially by Todd 1967 [6]. If buoyancy plays a role the situation is more complex. A better understanding of these effects is required for interpretation of data of future 3D simulations or upcoming experiments.

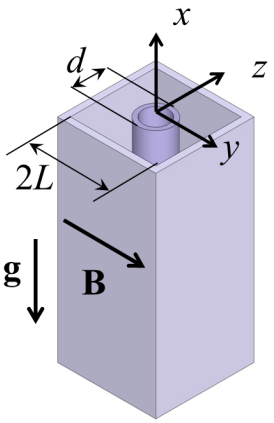

Fig. 2. Sketch of model geometry and coordinates. A circular cooling pipe is inserted into a liquid metal filled rectangular channel.

2. Formulation and scaling

The fluid in a long poloidal duct with cooling pipe is exposed to an externally applied uniform toroidal magnetic field $\mathbf{B} = B_0\hat{\mathbf{y}}$. The flow is driven either by an imposed pressure gradient or by buoyancy forces due to temperature gradients caused by the volumetric heat source in the fluid and cooling pipe. Density changes due to temperature variation in the liquid metal, which give rise to convective motions, are described by the Boussinesq approximation. The equations describing the problem are those accounting for a balance of momentum and conservation of mass:

$$\rho\frac{D\mathbf{v}}{Dt} = -\nabla p + \rho\nu\nabla^2\mathbf{v} - \rho\beta(T - T_0)\mathbf{g} + \mathbf{j}\times\mathbf{B}, \quad (1)$$

$$\nabla\cdot\mathbf{v} = 0. \quad (2)$$

Here $\mathbf{v}$ stands for velocity and p for deviation of pressure from isothermal hydrostatic conditions at the reference temperature T_0. The vector $\mathbf{g} = -g\hat{\mathbf{x}}$ denotes gravitational acceleration and $\mathbf{j}\times\mathbf{B}$ is the Lorentz force due to the interaction of electric current density $\mathbf{j}$ and magnetic field $\mathbf{B}$. The current

density $\mathbf{j}$ is determined via Ohm's law and charge conservation,

$$\mathbf{j} = \sigma(-\nabla\phi + \mathbf{v} \times \mathbf{B}),\ \nabla \cdot \mathbf{j} = \mathbf{0}, \tag{3}$$

which result in a Poisson equation for electric potential ϕ

$$\nabla \cdot \nabla\phi = \nabla \cdot (\mathbf{v} \times \mathbf{B}). \tag{4}$$

The physical properties of the fluid, such as the density ρ, the kinematic viscosity ν, the volumetric thermal expansion coefficient β, and the electric conductivity σ [7] are assumed constant in the temperature range considered and taken at reference temperature T_0.

The distribution of temperature T in the fluid is determined by the energy balance equation

$$\rho c_p \frac{DT}{Dt} = k\nabla^2 T + Q, \tag{5}$$

where c_p is the specific heat of the fluid at constant pressure, k the thermal conductivity and Q a volumetric heat source.

For the considered model-problem the volumetric heating Q is assumed to be constant, external duct walls are adiabatic and the central pipe is maintained at constant temperature T_0. All solid walls are electrically insulating and the no-slip condition $\mathbf{v} = 0$ applies.

For fully developed conditions the convective heat flux in (5) and inertial terms in (1) vanish, the velocity becomes unidirectional and the pressure gradient becomes constant with orientation along the duct axis,

$$\mathbf{v} = u_0 u\,(y, z)\,\hat{\mathbf{x}},\quad \nabla p = -\sigma u_0 B_0^2\ \pi\hat{\mathbf{x}}. \tag{6}$$

In (6) $u\,(y, z)$ and π stand for nondimensional velocity and pressure gradient. Temperature variations in the plane of the cross section are described by the dimensionless temperature $\theta\,(y, z)$ according to

$$T = T_0 + \theta\,(y, z)\,\Delta T, \tag{7}$$

where $\Delta T = QL^2/k$ is used as characteristic temperature difference. The length scale L corresponds to the Hartmann length of the duct (Fig. 2). The scale for velocity u_0 is either chosen as the average velocity in the duct cross section for pressure driven flows or as $u_0 = \nu/L\ Gr/Ha$ for buoyant MHD flows in insulating ducts. Due to the linearity of the problem any mixed convection case can be achieved as linear superposition of pure forced flow and free convection.

The flow is characterized by two dimensionless groups, the Hartmann number Ha, which is a nondimensional measure for the strength of the magnetic field, and the Grashof number Gr as a buoyancy parameter,

$$Ha = B_0 L\sqrt{\frac{\sigma}{\rho\nu}},\quad Gr = \frac{g\beta L^3 \Delta T}{\nu^2}. \tag{8}$$

3. Numerical results

Numerical simulations have been performed by means of a finite volume code developed on the basis of the software package OpenFOAM [8]. Equations describing the magnetohydrodynamic flow, (1)-(5), have been implemented. The current density conservative scheme proposed in [9] is employed and pressure-velocity coupling is accomplished by a PISO algorithm. The central difference scheme has been used for spatial discretization, while temporal discretization is first order accurate.

3.1. *Pressure driven flows*

In a first series of simulations velocity, potential and current distributions have been determined for pressure driven MHD flows in the model geometry. Figure 3 shows contours of potential and streamlines of electric current density for a relatively small Hartmann number $Ha = 10$. The topology of current density consists of closed current recirculations near the corners and above and below the pipe. There exists a well defined region around the pipe from which currents cannot escape. It is interesting to observe how the current patterns modify when Ha increases. A comparison with results for $Ha = 1000$ (Fig. 4) shows that the flow develops uniform cores to the right and left (C_r and C_l) and other cores above and below the pipe (C_p). The cores are separated from each other by tangent layers of thickness $\delta_t \sim Ha^{-1/2}$ that spread along magnetic field lines. At the right and left duct wall we find the well-known parallel Shercliff layers of thickness $\delta_s \sim Ha^{-1/2}$. The Hartmann layers with thickness $\delta_H \sim Ha^{-1}$ at Hartmann walls, where the magnetic field has a normal component, are so thin that they are not visible in the figure. Although both figures look quite different from a first point of view, the overall topology remains unchanged. With increasing Ha the critical points move closer to the Hartmann walls and the two saddle points at $y = 0$ move into the tangent layer. Closed current recirculations are present above and below the pipe in C_p, involving roughly half the cores, the tangent layers and the Hartmann layers at the pipe (inside closed blue loop). The four

areas enclosed by the red limiting streamlines represent other regions with locally closed current recirculations, mainly located in the outer cores C_r and C_l with current closure through the Shercliff, Hartmann and tangent layers. Current lines that involve and couple all different cores C_r, C_p, C_l across the tangent layers are those located between the red and blue loops. Current closure here is completed along Shercliff and Hartmann layers. A comparison with the sketch of currents for circular concentric pipes also shows the closed recirculations above and below the pipe but the other four loops cannot be seen in reference [6].

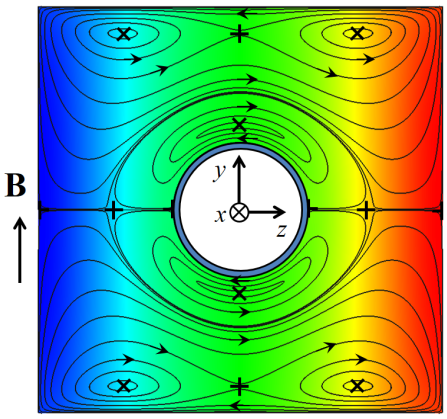

Fig. 3. Contours of potential ϕ and electric current streamlines for pressure driven flows at $Ha = 10$. Critical points in the topology are vortex centers $\times$, saddle points $+$, and half saddles $\dashv$.

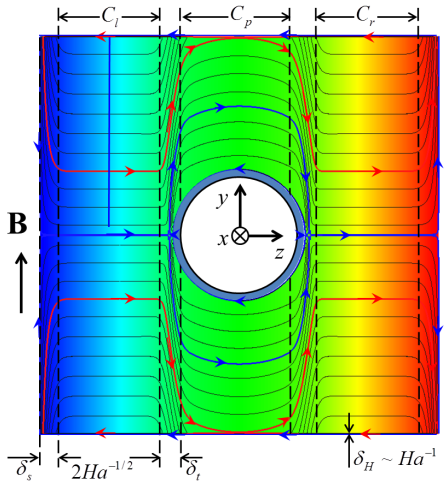

Fig. 4. Contours of potential ϕ and electric current streamlines for pressure driven flows at $Ha = 1000$.

Profiles of velocity are shown for a $Ha = 10$ and $Ha = 1000$ in Figs. 5,6. We observe for both Hartmann numbers in all cores uniform velocities along magnetic field direction y with thin viscous Hartmann layers at the duct walls and pipe. In transverse direction z the velocity in the outer cores is also uniform while in the inner cores u shows some dependence on z. It is interesting to notice that the velocity profiles in both cases are quite similar (apart from the thickness of Hartmann layers, since δ_H varies as Ha^{-1}) although the current distributions show significant differences.

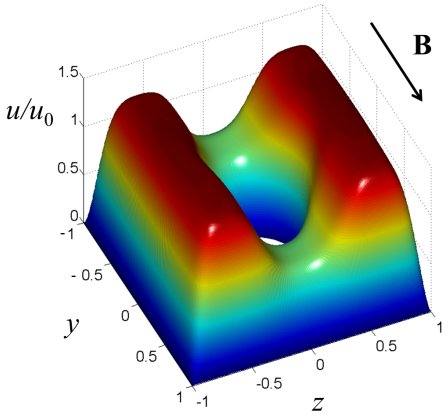

Fig. 5. Axial velocity profile for pressure driven flows at $Ha = 10$.

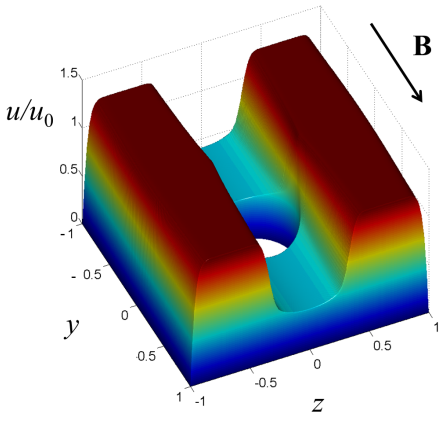

Fig. 6. Axial velocity profile for pressure driven flows at $Ha = 1000$.

3.2. *Buoyant flows*

In the following it is assumed that the flow is purely driven by buoyancy, i.e. we consider a long rectangular closed cavity filled with a volumetrically

heated fluid. The latter is cooled by a central circular pipe. In this case the average velocity in a cross section is zero. At some distance from the ends of the cavity temperature is independent of the flow and uniquely described by $\theta\,(y,z)$, contours of which are shown in the lower half of Fig. 7 for the flow at $Ha = 10$. Around the cooling pipe the isotherms form nearly concentric circles. From a hydrodynamic point of view it is expected that the cold fluid around the pipe moves downward, while the hot fluid near the outer walls moves upward. This is in fact almost the case for low Hartmann numbers as displayed in the Figs. 7, 8. This behavior, however, changes completely for higher magnetic fields. While the temperature field and resulting buoyancy forces remain unaffected as in Fig. 7, the regions of high downward velocity detach from the pipe and align themselves along magnetic field lines, forming tangent layers (see Figs. 9, 10 for $Ha = 1000$). It is interesting to notice that even if there exists a radial distribution of θ the velocity has a tendency to form uniform cores along y, i.e. the flow exhibits a sort of quasi two-dimensional state. The highest downward velocities are observed in the tangent layers, where the fluid moves down even in regions where buoyancy points upward. Electric current paths become quite complex for higher Ha as displayed in Fig. 9. While for $Ha = 10$ currents close preferentially in the bulk of the fluid, for $Ha = 1000$ practically all currents pass through the Hartmann layers. We have seen that in pressure driven flows a significant amount of current flows along the tangent layers but for buoyant flows currents just cross these layers.

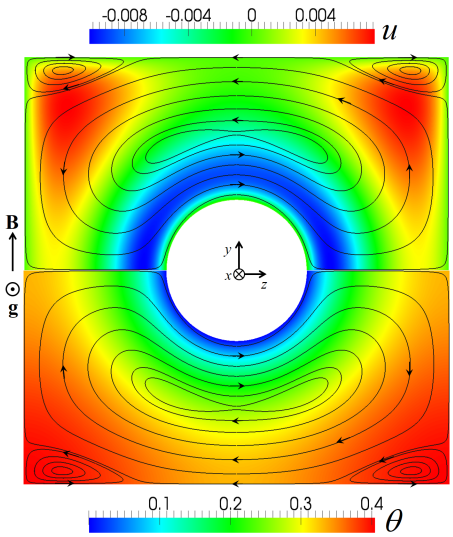

Fig. 7. Distribution of temperature (lower half) and of vertical velocity (upper half) for buoyancy driven flow at $Ha = 10$. Electric current streamlines are shown as well.

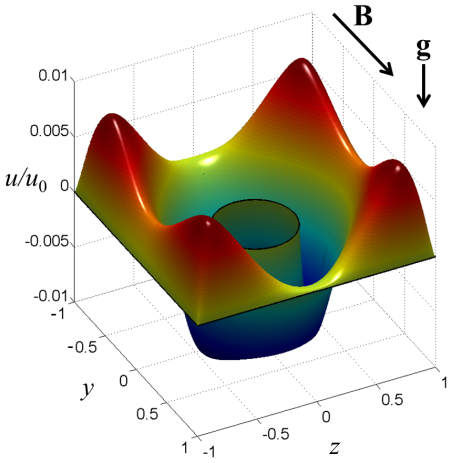

Fig. 8. Axial velocity profile for buoyancy driven flows at $Ha = 10$.

4. Conclusions

MHD flows in a model geometry for a WCLL blanket [2] have been analyzed numerically. The geometry consists of a long (poloidal) box, where one cooling pipe has been inserted as an internal obstacle. Two fundamental cases have been considered. The first is a pressure driven forced flow, which is required in WCLL blankets for slowly circulating the liquid metal to ancillary systems for tritium removal. For $Ha \gg 1$ the flow exhibits several cores with jumps in core velocity across thin internal tangent layers that provide a closure path for induced electric currents. The second investigated case is the buoyancy driven flow. Here electric current paths in the cores become quite complex, while the velocity tends towards a quasi-2D state. A significant amount of fluid is carried downward by the tangent layers. Future numerical studies will complement the results for electrically conducting walls and show at which values of Gr these layers will become possibly unstable. Flows in horizontal ducts as proposed in another design concept of a WCLL blanket [3] will be also studied.

Acknowledgment: This work has been carried out within the framework of the EUROfusion Consortium and has received funding from the Euratom research and training programme 2014-2018 under

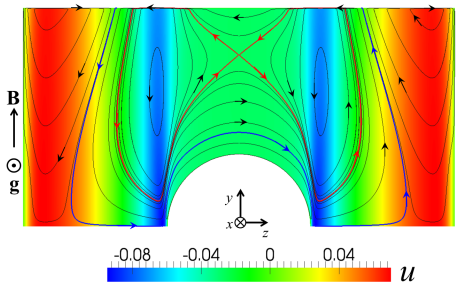

Fig. 9. Contours of axial velocity u and electric current streamlines for pressure driven flows at $Ha = 1000$ displayed in the upper half of the duct.

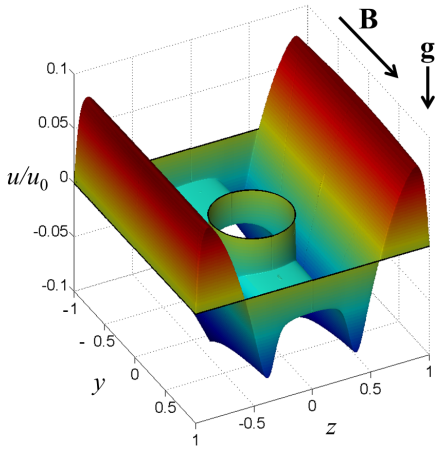

Fig. 10. Axial velocity profile for buoyancy driven flows at $Ha = 1000$.

grant agreement No 633053. The views and opinions expressed herein do not necessarily reflect those of the European Commission.

References

[1] F. Romanelli, P. Barabaschi, D. Borba, G. Federici, L. Horton, R. Neu, and et al. Fusion electricity: A roadmap to the realisation of fusion energy. Technical Report ISBN 978-3-00-040720-8, EFDA, 2012.

[2] J. Aubert, G. Aiello, N. Jonqures, A. Li Puma, A. Morin, and G. Rampal. Development of the water cooled lithium lead blanket for DEMO. *Fusion Engineering and Design*, 89(7-8):1386 – 1391, 2014.

[3] P.A. Di Maio, P. Arena, G. Bongiov, P. Chiovaro, A. Del Nevo, and R. Forte. Optimization of the breeder zone cooling tubes of the DEMO water-cooled lithium lead breeding blanket. *Fusion Engineering and Design*, 109-111:227–231, 2016.

[4] C. Mistrangelo and L. Bühler. Numerical study of fundamental magneto-convection phenomena in electrically conducting ducts. *IEEE Transactions on Plasma Science*, 40(3):584 – 589, 2012.

[5] C. Mistrangelo, Bühler, and G. Aiello. Buoyant-MHD flows in HCLL blankets caused by spatially varying thermal loads. *IEEE Transactions on Plasma Science*, 42(5):1407–1412, 2014.

[6] L. Todd. Hartmann flow in an annular channel. *Journal of Fluid Mechanics*, 28:371–384, 1967.

[7] U. Jauch, V. Karcher, B. Schulz, and G. Haase. Thermophysical properties in the system Li-Pb. Technical Report KfK 4144, Kernforschungszentrum Karlsruhe, 1986.

[8] C. Mistrangelo and L. Bühler. Development of a numerical tool to simulate magnetohydrodynamic interactions of liquid metals with strong applied magnetic fields. *Fusion Science and Technology*, 60(2):798–803, 2011.

[9] M.-J. Ni, R. Munipalli, N. B. Morley, P. Huang, and M. A. Abdou. A current density conservative scheme for incompressible MHD flows at a low magnetic Reynolds number. Part I: On a rectangular collocated grid system. *Journal of Computational Physics*, 227(1):174–204, 2007.